The Canadian Mineralogist
Vol. 50, pp. 281-294 (2012)
DOI: 10.3749/canmin.50.2.281

ELDRAGÓNITE, $Cu_6BiSe_4(Se_2)$, A NEW MINERAL SPECIES FROM THE EL DRAGÓN MINE, POTOSÍ, BOLIVIA, AND ITS CRYSTAL STRUCTURE

WERNER H. PAAR[§]

Pezoltgasse 46, A–5020 Salzburg, Austria

MARK A. COOPER

Department of Geological Sciences, University of Manitoba, Winnipeg, Manitoba R3T 2N2, Canada

YVES MOËLO

Institut des Matériaux Jean Rouxel (IMN), Université de Nantes, CNRS, 2, rue de la Houssinière, F–44322 Nantes, Cedex 3, France

CHRIS J. STANLEY

Department of Mineralogy, The Natural History Museum, Cromwell Road, London SW7 5BD, U.K.

HUBERT PUTZ AND DAN TOPA

Department of Materials Engineering and Physics, University of Salzburg, Hellbrunnerstr. 34, A–5020 Salzburg, Austria

ANDREW C. ROBERTS AND JOHN STIRLING

Geological Survey of Canada, 601 Booth Street, Ottawa, Ontario K1P 6P4, Canada

JOHANN G. RAITH

Department of Applied Geosciences and Geophysics, Montanuniversität, Peter Tunner Strasse 5, A–8700 Leoben, Austria

RALPH ROWE

Canadian Museum of Nature, P.O. Box 3443, Station D, Ottawa, Ontario K1P 6P4, Canada

ABSTRACT

Eldragónite, with the simplified formula $Cu_6BiSe_4(Se_2)$, is a new mineral species discovered in a telethermal vein-type deposit with selenides at the El Dragón mine, Province of Quijarro, Department of Potosí, Bolivia. It forms inclusions in kruťaite, and is associated with clausthalite, klockmannite, umangite and tiemannite, as well as with watkinsonite, petrovicite and two unnamed phases in the system Cu–Pb–Hg–Bi–Se. The unique vein of eldragónite-bearing kruťaite is hosted within sandstones and shales of Devonian age. Eldragónite occurs in anhedral grains and polycrystalline aggregates attaining a size of up to 100 × 80 μm. Megascopically, the mineral has a brownish to light-maroon color, is opaque and lacks internal reflections. It has a metallic luster and a brownish black streak, is brittle with an uneven to conchoidal fracture, without observable cleavage. The VHN_{15} values range between 212 and 243 (mean 225) kg/mm^2, corresponding to a Mohs hardness of ~3 ½. In plane-polarized light, eldragónite is distinctly bireflectant and pleochroic, from light grayish brown to cream; it is strongly anisotropic with rotation tints in shades of orange and blue-black. The reflectances (in air and oil, respectively) for the COM standard wavelengths are: 32.5–34.5, 17.7–19.7 (470 nm), 32.95–36.3, 18.0–21.4 (546 nm), 33.3–36.8, 18.3–21.6 (589 nm), 34.0–36.9, 19.1–21.7 (650 nm). Electron-microprobe analyses gave (mean of 24 analyses): Cu 35.9, Fe 1.25, Ni 0.35, Bi 20.3, Se 42.5, total 100.3 wt.%, corresponding to $(Cu_{5.98}Fe_{0.24}Ni_{0.06})_{\Sigma 6.28}Bi_{1.03}Se_{5.70}$. The ideal formula is $Cu_6BiSe_4(Se_2)$, which requires Cu 35.84, Bi 19.64,

§ *E-mail address*: paarwerner@aon.at

Se 44.52 wt.%. Eldragónite has an orthorhombic cell, space group *Pmcn*, with *a* 4.0341(4), *b* 27.056(3), *c* 9.5559(9) Å, *V* 1043.0(3) $Å^3$, and $Z = 4$. The calculated density is 6.76 g/cm^3. The strongest X-ray powder-diffraction lines [*d* in Å (*I*) *hkl*] are: 6.547(58)031, 3.579(100)052, 3.253(48)141, 3.180(77)081, 3.165(56)013, 3.075(84)102, 3.065(75)151,112, 2.011(53)200, 1.920(76)154, 1.846(52)1$\underline{10}$3. The crystal structure was solved from single-crystal data, and was refined to R_1= 0.026 on the basis of 1731 unique reflections. There are one Bi and six Cu positions. Among the six Se positions, two Se atoms form a Se_2 pair [d(Se–Se) = 2.413 Å]; eldragónite is thus a mixed selenide–diselenide compound. The crystal structure is organized according to two slabs alternating along **a**. The thin slab with formula Cu_6Se_6 is a zigzag layer derived from the CaF_2 archetype; the thick slab, $Cu_6Bi_2Se_6$, is similar to that of wittichenite, Cu_3BiS_3. The Se_2 pair is at the junction between these two slabs. This new mineral species is named after the location where it was discovered.

Keywords: eldragónite, copper, bismuth, selenium, diselenide, new mineral species, crystal structure, El Dragón mine, Quijarro, Potosí, Bolivia.

Introduction

The Andean mountain ranges of Bolivia and Argentina are well known for various deposits of selenium mineralization. Bolivia is famous for two selenide occurrences: El Dragón, province of Quijarro, and Pacajake, in the district of Hiaco de Charcas, both in the Department of Potosí. At El Dragón, Grundmann *et al*. (1990) described a single vein composed of almost massive krut̓aite ($CuSe_2$) associated with a great variety of other selenides that had probably been explored for its gold content. At Pacajake, an ore assemblage of penroseite ($NiSe_2$), naumannite (Ag_2Se) and clausthalite (PbSe), with contents of gold and platinum-group elements (PGE) was exploited for silver during the 1920s (Ahlfeld 1941, Ahlfeld & Schneider-Scherbina 1964, Block & Ahlfeld 1937, Redwood 2003, Kempff *et al*. 2003, 2009).

In the context of ongoing work at the Porco Ag–Pb–Zn deposit by two of the authors (WHP & HP), an excursion to the El Dragón mine was made in 2004. At that time, only insignificant remnants of the original krut̓aite vein were still exposed. A small dump, with high-grade and walnut-sized krut̓aite specimens in front of the entrance, yielded eldragónite in sufficiently large grains to characterize the new species, including a determination of its crystal structure.

A compound with similar optical properties and chemical composition to eldragónite was mentioned by Grundmann *et al*. (1990) from El Dragón. No data about the X-ray crystallography were published, probably because the material was not suitable for this purpose.

Probably the most extensive selenium province on Earth, however, is situated in the Argentinian province of La Rioja, where exploration of and exploitation for silver, mercury, gold and selenium are documented from areas such as Cerro de Cacho ("Sierra de Umango"; Brodtkorb & Crosta 2010), Los Llantenes and the Sierra de Famatina near Puerto Alegre ("Sañogasta"). The bulk of the Argentinian selenium mineralization is dominated by copper selenides (umangite, Cu_3Se_2, klockmannite, CuSe, and berzelianite, Cu_2Se) and tiemannite, HgSe. Contents of silver, gold and PGE (platinum, palladium) are valuable associates in the veins, and present as the minerals naumannite, Ag_2Se, eucairite, AgCuSe, native gold, Au, fischesserite, Ag_3AuSe_2 and chrisstanleyite, $Ag_2Pd_3Se_4$, jagüéite, $Cu_2Pd_3Se_4$ and merenskyite, $PdTe_2$ (Amann *et al*. 1999, Brodtkorb *et al*. 1990, 1993, Guerrero 1969, Paar *et al*. 1996a, 1996b, 1998a, 1998b, 2000, 2002a, 2002b, 2004a, 2004b, 2004c, 2004d).

At the San Francisco mine near Puerto Alegre, province of La Rioja, Argentina, another Cu–Bi–Se compound had been observed as inclusions in umangite in minor amounts (Brodtkorb, M.K. de, pers. commun.). The optical properties and the chemical composition very much resemble eldragónite, but no X-ray data are available.

The new mineral species eldragónite, $Cu_6BiSe_4(Se_2)$, and its name have been approved by the Commission on New Minerals, Nomenclature and Classification (CNMNC), IMA, proposal 2010–077. The holotype, which is the pre-analyzed crystal used for the determination of the crystal structure, is deposited in the collections of the Canadian Museum of Nature, Ottawa, Canada, and registered under CMNMC 86154. Cotype specimens of eldragónite-bearing krut̓aite are housed within the reference collections of the Department of Materials Engineering and Physics, University of Salzburg, Austria, and numbered as M 17.001, 17.002 and 17.003.

Location and Geology

The El Dragón mine is located some 30 km southwest of Cerro Rico at Potosí, thus in one of the most famous silver–tin mining districts of Bolivia. The coordinates of the only adit of this mine are 19°49.15' South and 65°55' West, and its altitude is ~4100 m above sea level. The mine can be reached from Potosí in two and a half hours, passing the village of Agua Castilla, which is close to the large underground mine at Porco. A gravel road ends at the village of Sala Khuchu, from where a trail leads up to the mine (Fig. 1).

The single selenide vein in this telethermal deposit is hosted by sandstones and shales (Grundmann *et al*. 1990, Ahlfeld & Schneider-Scherbina 1964) of Devonian age. Reddish sandstones of probably Permian age and thick andesitic lava flows also occur in the area.

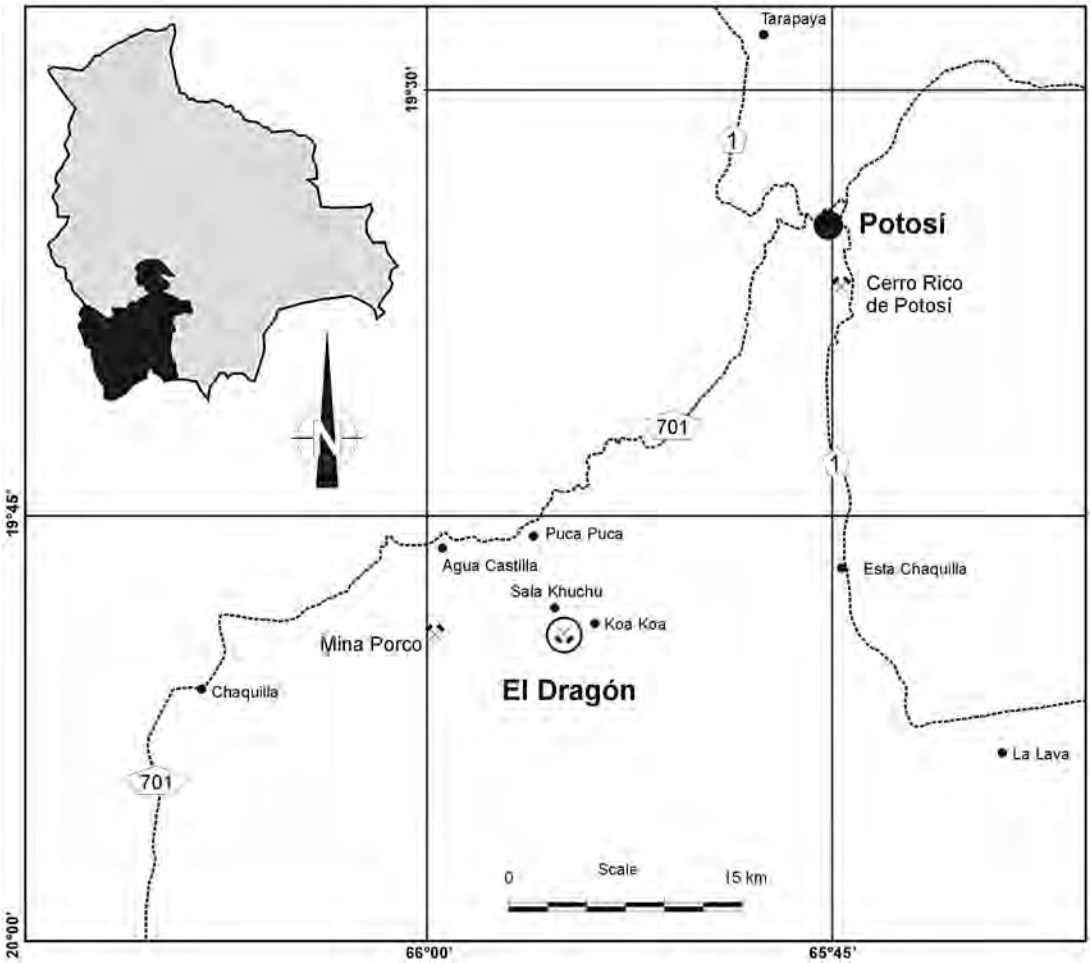

FIG. 1. Location map of the El Dragón mine, Department of Potosí, Bolivia.

According to a very detailed study by Grundmann *et al*. (1990), the single vein as it was exposed during their stay had a thickness ranging from 0.5 to 2 cm with a local increase up to 6 cm. The vein follows a distinct structure and could be traced along strike for at least 10 m. A continuation with depth can be assumed, but would have to be substantiated through development work. Several specimens of massive kruťaite containing abundant eldragónite, obtained from H. Wotruba (Aachen University, Germany), show a very distinct brecciation of the ore, with angular fragments of kruťaite embedded in a distinctly altered matrix.

ELDRAGÓNITE AND THE SELENIDE MINERALIZATION

Eldragónite is a widespread constituent of the selenide assemblage and is invariably included in chemically zoned kruťaite (Figs. 2a–c). Grundmann *et al*. (1990) carried out a very detailed study of the chemical composition of this mineral, which nearly spans the entire range between the end-member compositions kruťaite ($CuSe_2$) and penroseite ($NiSe_2$). In addition, Co-bearing kruťaite was observed, but members plotting in the field of trogtalite ($CoSe_2$) were not identified.

Eldragónite seems to be more common in those types of kruťaite ore that have undergone a late event of brittle deformation, causing brecciation. Subsequent infiltration of fluids containing bismuth, lead and mercury led to the precipitation of clausthalite, watkinsonite, petrovicite and related unnamed phases.

Eldragónite can be found concentrated in random sections of kruťaite crystals (Fig. 2a) where these are embedded in a carbonate gangue. Commonly irregularly shaped, and also elongate, aggregates of eldragónite

grains follow distinct growth-zones within kruťaite (Fig. 2a), replacing a Co-rich member of the series trogtalite – penroseite – kruťaite.

Eldragónite is commonly associated with watkinsonite (Fig. 2b), present as bent lamellae up to several hundred μm in length. Petrovicite (Fig. 2c) is less common as anhedral grains that can reach 100 × 60 μm. Two unnamed compounds of the system Cu–Pb–Hg–Bi–Se were found in two polished sections. Their sizes are too small for those grains to be extracted for an X-ray study. Both phases (phase "A" and phase "B") occur in veinlets up to a width of 100 μm within kruťaite. Phase "A" is associated with clausthalite, phase "B" not. Phase "A" forms lath-shaped crystals that attain a length of up to 50 μm and a width ranging between 5 and 10 μm. The associated minerals are watkinsonite and klockmannite, which fill interstices between the laths of phase "A". Optically, phase "A" is distinctly anisotropic with bluish to greenish rotation-tints; lamellar twinning is common. Phase "B" is closely associated with phase "A" and forms irregular intergrowths of anhedral grains within phase "A". Optically, phase "B" is anisotropic but lacks the colorful rotation-tints of "A"; no twinning was observed.

Clausthalite (PbSe) is next in abundance after kruťaite, and commonly observed as a network penetrating the hosting kruťaite. Watkinsonite and petrovicite occasionally can be found embedded in this veining of clausthalite.

Klockmannite (CuSe) and umangite (Cu_3Se_2) are fairly abundant. The former occurs in aggregates of tabular crystals up to several 100 μm, the latter in tiny grains and grain clusters disseminated throughout the kruťaite matrix. Tiemannite (HgSe) was detected only once. Berzelianite (Cu_2Se) and eskebornite ($CuFeSe_2$), which were mentioned by Grundmann *et al.* (1990), are not present in our material.

Native gold can be detected in almost every section, in varying shapes and grain sizes, commonly exceeding 100 μm. Sulfide minerals (chalcopyrite, pyrite, marcasite, covellite and phases belonging to the system Cu–S) predate the selenium mineralization. Traces of native selenium and various secondary phases (goethite, chalcomenite, olsacherite, schmiederite, cobaltomenite and ahlfeldite) are ubiquitous in the oxidized material.

Physical and Optical Properties

Eldragónite usually occurs as very irregularly shaped grains and grain clusters that attain a size of 100 × 80 μm. The majority of the grains, however, are much smaller and range in size between 10 and 50 μm. Almost all grains are not "single crystals" but polycrystalline aggregates. Even the grain used for the study of the crystal structure turned out to be an intergrowth of differently oriented crystals.

Eldragónite has a brownish to light maroon color, which is enhanced by the contrast with the kruťaite matrix. The mineral is opaque, has a metallic luster and a brownish black streak. It is brittle with an uneven to conchoidal fracture. Neither cleavage nor parting was observed. The mineral is non-fluorescent. The VNH_{15} values measured from eight indentations range between 212 and 243 (mean 224) kg/mm^2, thus corresponding to a Mohs hardness of ~3½ (Young & Millman 1964).

The density could not be measured because of the intimate interfingering of the larger grains with the enclosing matrix. The density calculated on the basis of the empirical formula and $Z = 4$ is 6.76 g/cm^3. Wittichenite (Cu_3BiS_3) and skinnerite (Cu_3SbS_3), which have some structural features comparable to those of eldragónite, have a density of 6.01 and 5.1 g/cm^3, respectively.

In plane-polarized light, eldragónite is distinctly bireflectant and pleochroic, from light grayish brown to cream in its association with kruťaite, colors that are enhanced in oil immersion. In crossed polars, it is strongly anisotropic, with rotation tints in shades of orange to blue-black with an undulose extinction. Internal reflections are absent.

Quantitative reflectance values were obtained at the Natural History Museum, London, on a Zeiss Axiotron microscope equipped with a J & M Tidas diode array spectrometer run by Cavendish Instruments Onyx software. After careful leveling of the specimen and standard (Zeiss, SiC standard number 472) using a Lanham leveling stage, measurements were taken at intervals of about 0.82 nm from 400 to 700 nm in air and in oil immersion (index of refraction $n = 1.515$). The results are presented in Table 1 and presented graphically in Figure 3. Color values were calculated from the tabulated datasets.

From 400 to ~700 nm, the reflectance values of R_1 are continuously ascending toward the longer wavelengths. The values for R_2 show a more rapid increase between 400 and 600 nm, but then are constant between 600 and 700 nm. The increase in the reflectances and in the bireflectance toward the longer wavelengths is consistent with the color and the optical properties of eldragónite.

Chemical Composition

Eldragónite

Quantitative chemical analyses for eldragónite were carried out at the Eugen F. Stumpfl electron-microprobe laboratory installed at the Department of Geosciences, Institute of Mineralogy & Petrology, University of Leoben, Austria. A JEOL JXA 8200 electron microprobe was used, operated at 20 kV, 10 nA, and 20 s counting time for peak and 10 s for background, with a beam diameter of 2 μm. The following natural (n) and synthetic (s) standards, and the emission lines are: n chalcopyrite (Cu*K*α), n pyrite (Fe*K*α, S*K*α), s NiAs (Ni*K*α), s Bi_2Se_3 (Bi*L*α) and s CuSe (Se*K*α). The raw

data were corrected with the on-line ZAF–CITZAF (version 3.5) program.

The results show only slight grain-to-grain variation of the chemical composition of eldragónite in all the sections. A typical example of this variation is included in Table 2 and refers to the grain later used for the determination of the crystal structure. The empirical formula of eldragónite, normalized to 13 atoms per formula unit (*apfu*), is $(Cu_{5.98}Fe_{0.24}Ni_{0.06})_{\Sigma 6.28}Bi_{1.03}Se_{5.70}$. The simplified formula is $Cu_6BiSe_4(Se_2)$, which requires Cu 35.84, Bi 19.64 and Se 44.52, total 100 wt.%.

TABLE 1. REFLECTANCE DATA AND CALCULATED COLOR VALUES FOR ELDRAGÓNITE

	Air		Oil			Air		Oil	
λ (nm)	R_1 %	R_2 %	R_1 %	R_2 %	λ (nm)	R_1 %	R_2 %	R_1 %	R_2 %
400	32.0	32.6	17.2	17.9	560	33.0	36.5	18.1	21.5
420	32.1	32.8	17.4	18.1	580	33.2	36.7	18.2	21.6
440	32.2	33.4	17.5	18.7	**589**	**33.3**	**36.8**	**18.3**	**21.6**
460	32.3	34.1	17.6	19.3	600	33.4	36.8	18.4	21.65
470	**32.5**	**34.5**	**17.7**	**19.7**	620	33.7	36.9	18.7	21.7
480	32.6	34.9	17.7	20.1	640	33.9	36.9	19.0	21.7
500	32.8	35.5	17.8	20.6	**650**	**34.0**	**36.9**	**19.1**	**21.7**
520	32.9	35.9	17.9	21.1	660	34.1	36.9	19.2	21.7
540	32.95	36.2	18.0	21.4	680	34.4	36.9	19.3	21.7
546	**32.95**	**36.3**	**18.0**	**21.4**	700	34.6	37.0	19.4	21.8

Color values

	C illuminant				A illuminant			
x	0.314	0.317	0.315	0.32	0.451	0.453	0.453	0.454
y	0.319	0.325	0.32	0.33	0.408	0.411	0.408	0.413
Y %	33.1	36.3	18.1	21.3	33.2	36.5	18.3	21.5
λ_d	579	574	582	573	589	583	592	582
P_e %	1.7	4.2	2.4	6.4	2.6	5.9	3.7	8.6

Watkinsonite, petrovicite and unnamed phases

Electron-microprobe analyses of these rare phases were performed at the Department of Materials Engineering and Physics, University of Salzburg, Austria, utilizing a JEOL SUPERPROBE JXA–8600, controlled by the Probe for Windows system of programs operated in wavelength-dispersion (WDS) mode at 25 kV, a beam current of 20 nA, 15 s counting time for peaks and 5 s for background. Data correction was done on-line with the ZAF–4 program. The following standards and emission lines were used: n chalcopyrite (Cu*K*α, Fe*K*α), s Ag metal (Ag *L*α), n cinnabar (Hg*L*α), n galena (Pb*L*α), s Bi_2Se_3 (Bi*L*α, Se*K*α), s Bi_2S_3 (S*K*α) and s Te metal (Te*L*α). The results are included in Table 2.

The composition of watkinsonite, ideally $Cu_2PbBi_4(Se,S)_8$ (Topa *et al.* 2010), based on $\Sigma(M + SM + Se) = 15$, is $(Cu_{1.66}Ag_{0.31}Fe_{0.03})_{\Sigma 2}Pb_{1.10}Hg_{0.05}Bi_{4.02}(Se_{7.79}Te_{0.03})_{\Sigma 7.82}$ (mean of 14 analyses), thus making it a Ag-bearing variety of this rare sulfosalt. Petro-

TABLE 2. COMPOSITIONS OF ELDRAGÓNITE, ASSOCIATED PHASES (EL DRAGÓN) AND "Cu–Bi–Se" FROM SAN FRANCISCO MINE, ARGENTINA

No.	mineral	n[1]		Cu	Ag	Fe	Ni	Pb	Hg	Bi	Te	S	Se	Total
1	eldragónite	24	mean	35.9	-	1.3	0.4	-	-	20.3	-	-	42.5	100.4
	Mina El Dragón		s.d.[2]	0.27		0.12	0.15			0.2			0.3	
			min	35.1		1.0	-			19.9			41.9	
			max	36.5		1.4	0.6			20.7			43.0	
2	"Cu-Bi-Se" [3]	7	mean	35.5	-	-	-	-	-	19.2	-	-	44.2	98.9
	Mina		s.d.[2]	0.28						0.43			0.17	
	San Francisco		min	35.1						18.8			43.9	
			max	35.9						19.8			44.3	
3	"Cu-Bi-Se" [4]	15	mean	38.2	-	-	-	-	-	18.9	-	-	42.7	99.8
	Mina		s.d.[2]	0.84						0.91			0.55	
	San Francisco		min	37.1						17.8			42.3	
			max	40.6						19.8			44.4	
4	petrovicite	8	mean	15.5	0.5	-	-	17.3	16.9	17.2	-	-	31.1	98.6
	Mina El Dragón		s.d.[2]	0.68	0.26			0.36	0.34	0.64			0.35	
5	watkinsonite	14	mean	5.7	1.8	0.1	-	12.3	0.6	45.3	0.1	-	33.2	99.2
	Mina El Dragón		s.d.[2]	0.18	0.35	0.1		0.22	0.11	0.18	0.1		0.39	
6	"A"	3	mean	12.7	1.2	-	-	16.8	8.1	26.9	0.2	-	32.7	98.4
	Mina El Dragón		s.d.[2]	0.36	0.13			0.70	0.15	0.20	0.1		0.50	
7	"B"	4	mean	9.9	0.4	-	-	13.7	11.7	29.7	-	-	32.5	97.9
	Mina El Dragón		s.d.[2]	0.48	0.26			0.43	0.35	0.15			0.47	

[1] number of analyses; [2] standard deviation; [3] analyst: H.-J. Bernhard, [4] analyst: A. Martin-Izard. The compositional data, quoted in wt.%, were generated with an electron microprobe.

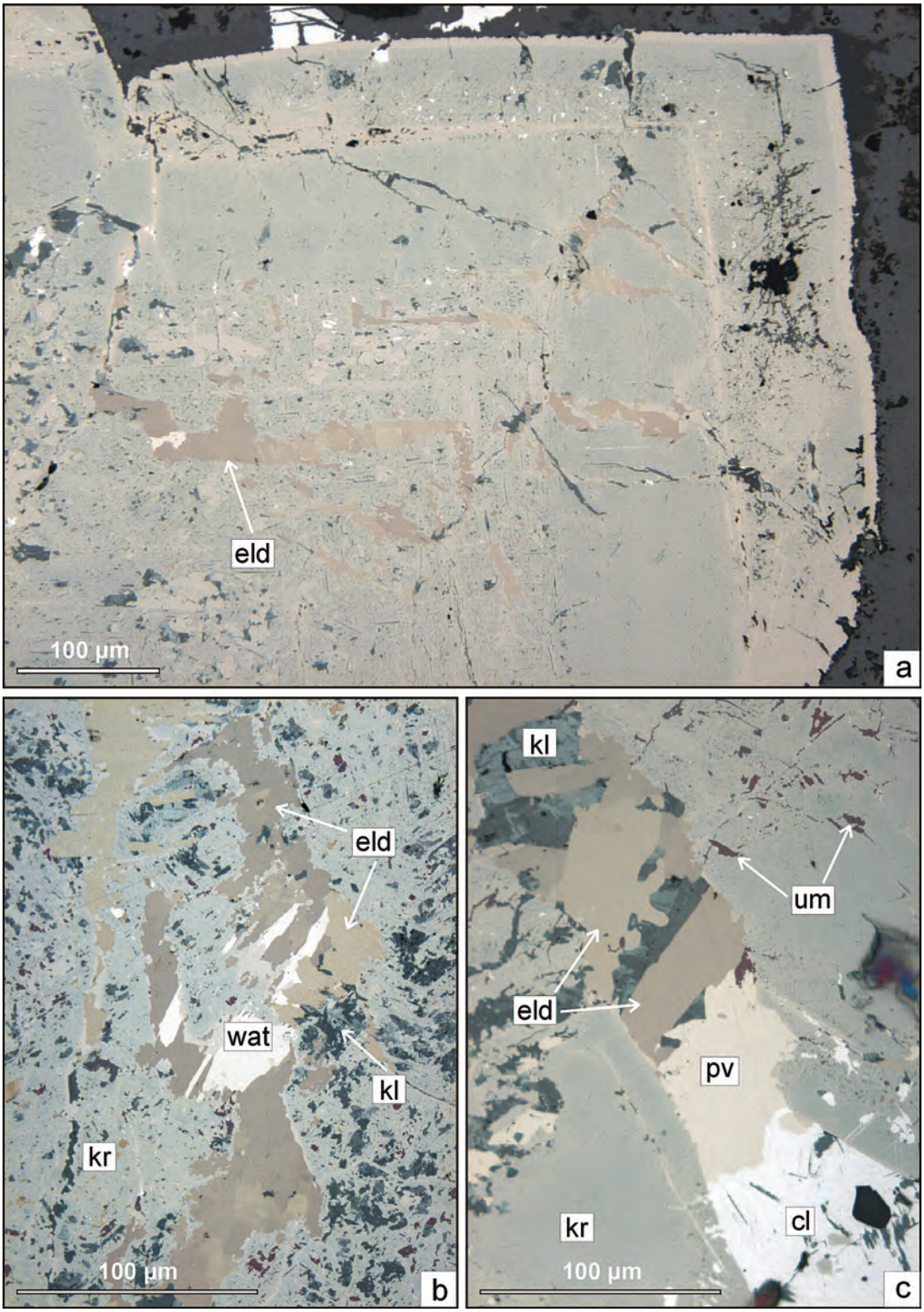
eld
100 µm
a
eld
wat
kl
kr
100 µm
b
kl
um
eld
pv
kr
cl
100 µm
c

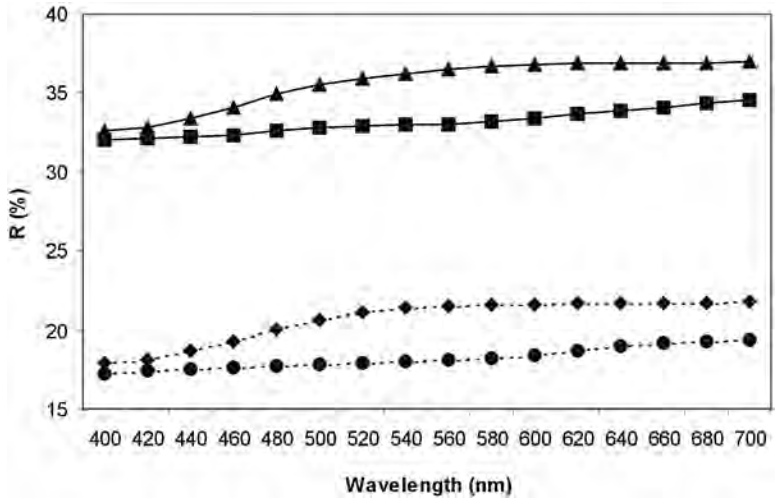

FIG. 3. Reflectance spectra of eldragónite. The data points are coded as follows: ■ air, R1; ▲ air, R2; ● oil, R1; ♦ oil, R2.

vicite, ideally $Cu_3HgPbBiSe_5$, has $(Cu_{3.00}Ag_{0.06})_{\Sigma 3.06}Hg_{1.04}Pb_{1.03}Bi_{1.01}Se_{4.85}$ (mean of 8 analyses), thus not deviating much from the ideal composition. The two unnamed phases, which belong to the system Cu–Hg–Pb–Bi–Se just as petrovicite, have the following chemical compositions: $(Cu_{4.80}Ag_{0.27})_{\Sigma 5.07}Hg_{0.97}Pb_{1.95}Bi_{3.09}Se_{9.90}$ (phase "A", ideally $Cu_5HgPb_2Bi_3Se_{10}$, mean result of three analyses) and $(Cu_{2.20}Ag_{0.05})_{\Sigma 2.25}Hg_{0.84}Pb_{0.95}Bi_{2.04}Se_{5.9}$ (phase "B", ideally $Cu_2HgPbBi_2Se_6$, mean result of four analyses).

X-RAY POWDER-DIFFRACTION DATA

Extraneous fines of micrometric crystals of eldragónite, collected during the cutting process necessary to liberate a suitable fragment for structure study, were attached to a conventional Debye–Scherrer powder mount and run on a Bruker microdiffractometer using Cu*K*α radiation (λ = 1.54178 Å). The fully indexed powder-diffraction data are presented in Table 3. The unit-cell parameters, *a* 4.024(2), *b* 27.014(9), *c* 9.544(3) Å, *V* 1037.6(7) Å^3, *a:b:c* = 0.1490:1:0.3533, were refined from 29 reflections representing *d* values between 6.547 and 1.818 Å for which unambiguous indexing was possible, on the basis of the calculated intensities derived from the crystal structure. The powder data are unique and bear no resemblance to any other inorganic phase listed in the Powder Diffraction File, and no synthetic equivalent is known in the chemical literature.

FIG. 2. a) Eldragónite (eld) as inclusions in distinctly zoned krut̀aite. Clausthalite is white. b) Inclusions of intergrown eldragónite and watkinsonite (wat) and klockmannite (kl), in krut̀aite. The very strong pleochroism of eldragónite is clearly visible. c) Veinlet of eldragónite intergrown with klockmannite (kl) and randomly associated with petrovicite (pv) and clausthalite (cl), in a matrix of krut̀aite (kr). Umangite (um) is disseminated throughout the matrix Plane-polarized light.

SINGLE-CRYSTAL STUDY

A single crystal (7 × 12 × 20 μm) was mounted on a Bruker D8 three-circle diffractometer equipped with a rotating anode generator (Mo*K*α X-radiation), multi-layer optics in the incident beam path, and an APEX–II CCD detector. A sphere of X-ray-diffraction data was collected to 60° 2θ using 60 s per 0.2° frame with a crystal-to-detector distance of 5 cm. The diffraction maxima display variable splitting consistent with a second crystalline component. The unit-cell parameters were obtained by least-squares refinement of 9896 reflections ($I > 10\sigma I$). Eldragónite has an orthorhombic cell with *a* 4.0341(4), *b* 27.056(3), *c* 9.5559(9) Å, *V* 1043.02 Å^3, space group *Pmcn* and *Z* = 4. The complete diffraction pattern was integrated using the orientation matrix of the dominant primary component and that of the subordinate second-crystal component (related by a 2.2° rotation about [1.000 –0.444 0.317]). At the completion of frame integration, there was a total of 68093 reflections (31435 belong to component #1, 30725 belong to component #2, and 5933 are composites). Data scaling (merging of identical reflections

TABLE 3. X-RAY POWDER-DIFFRACTION DATA FOR ELDRAGÓNITE

I_{rel}	d_{meas}	d_{calc}	h	k	l	I_{rel}	d_{meas}	d_{calc}	h	k	l
***58**	**6.547**	6.550	0	3	1	*22	2.484	2.485	1	1	3
24	4.501	4.502	0	6	0	*20	2.406	2.405	1	3	3
		4.499	0	2	2	*34	2.272	2.274	1	8	2
*22	4.217	4.217	0	3	2	*23	2.183	2.183	1	10	1
*20	4.071	4.072	0	6	1	*18	2.105	2.108	0	6	4
100	**3.579**	3.578	0	7	1	22	2.094	2.096	1	11	0
		3.577	0	5	2			2.096	1	7	3
		3.576	1	2	1	*36	2.028	2.029	1	2	4
*47	3.426	3.429	1	3	1	***53**	**2.011**	2.012	2	0	0
*27	3.273	3.275	0	6	2	***76**	**1.920**	1.919	1	5	4
*48	3.253	3.250	1	4	1	*27	1.905	1.905	0	13	2
***77**	**3.180**	3.183	0	8	1	*25	1.868	1.867	0	3	5
***56**	**3.165**	3.160	0	1	3	***52**	**1.846**	1.846	1	13	0
*40	3.090	3.097	0	2	3	*40	1.835	1.833	1	10	3
***84**	**3.075**	3.076	1	0	2	*22	1.815	1.813	1	13	1
75	3.065	3.057	1	5	1	16	1.723	1.722	1	13	2
		3.057	1	1	2			1.721	1	1	5
33	3.004	3.001	0	7	2	20	1.712	1.711	0	11	4
		3.000	0	3	3			1.711	0	7	5
38	2.865	2.863	0	9	1	17	1.703	1.701	2	8	1
		2.862	1	6	1			1.697	2	1	3
*13	2.804	2.800	1	4	2	15	1.642	1.646	2	9	1
*24	2.759	2.756	0	8	2			1.644	1	15	0
*41	2.745	2.741	0	5	3			1.635	1	14	2
*29	2.694	2.701	0	10	0	15	1.623	1.625	2	8	2
*48	2.671	2.674	1	7	1			1.622	2	5	3
*25	2.495	2.497	1	8	1						

Indexed with *a* 4.024(2), *b* 27.014(9), *c* 9.544(3) Å; *: lines used for unit-cell refinement. The d values are quoted in Å.

TABLE 4. CRYSTALLOGRAPHIC DATA AND REFINEMENT PARAMETERS FOR ELDRAGÓNITE

Crystal data	
Ideal formula	$Cu_6BiSe_4(Se_2)$
Crystal system	orthorhombic
Space group	*Pmcn*
Unit-cell parameters *a*, *b*, *c* (Å)	4.0341(4), 27.056(3), 9.5559(9)
Unit-cell volume (Å^3)	1043.0(3)
Z	4
Crystal size (μm)	7 × 12 × 20
Volume ratio of the single crystal	62%
Data collection	
Diffractometer	Bruker D8
Temperature (K)	294
Radiation, wavelength (Å)	Mo*K*α, 0.71073
θ range for data collection (°)	1 – 30.00
h, *k*, *l* ranges	± 5, ± 38, ± 13
frame width (°), frame time (s)	0.2, 60
Total reflections collected	68093
Unique reflections (R_{int})	1731 (0.053)
Unique reflections $F > 4\sigma(F)$	1569
Method of absorption correction	TWINABS
Structure refinement	
Refinement method	Full-matrix least-squares on F^2
Data / restraints / parameters	1731/0/86
R_1 [$F_o > 4\sigma(F_o)$]	0.0263
R_1 all	0.0320
Goodness-of-fit on F^2	1.213
Largest diff. peak and hole (e$^-$/Å^3)	1.54, –2.14

collected at multiple diffraction-vector settings) and Laue merging (μ) resulted in a total of 4448 unique reflections (components #1 + #2 + composites). The final intensity-data file (HKLF 5 format) consists of 2626 reflections (component #1 + composites).

The structure was solved by direct methods and refined by full-matrix least-squares method SHELXL–97 (Sheldrick 1997). Systematically absent reflections are consistent with the space group *Pmcn*. The structure was initially solved using this space group, and an HKLF 4 data file that contained only resolved component #1 reflections. For the final refinement model, we used the HKLF 5 data file that includes the contribution of the second component to the composite reflections. A fully anisotropic refinement model was refined to $R_1 = 2.6\%$, and contains 38% by volume of the second component fraction [BASF = 0.383(3)].

Table 4 gives crystallographic data and refinement parameters for eldragónite. Tables 5 and 6 give coordinates, isotropic and anisotropic displacement parameters of all atoms. A list of structure factors and a cif file are available from the Depository of Unpublished Data, on the Mineralogical Association of Canada website (document Eldragónite CM50_281).

Description of the Crystal Structure

Unit-cell content and cation coordination

In Figure 4, we present a projection of the unit cell of the structure of eldragónite along **a**. There are one Bi, six Cu and six Se positions. Table 7 gives bond distances in the structure of eldragónite. Atoms Se1 and Se5 form a (Se–Se) pair, with a short bond (2.413 Å) close to the (Se–Se) distance of trigonal Se (2.375 Å: Keller *et al.* 1977). The Bi atom has a dissymmetric coordination (Fig. 5), with three short distances (2.708 and 2 × 2.791 Å) and two of intermediate length (2 × 3.242 Å) forming a distorted square pyramid, completed by two longer bonds (2 × 3.540 Å). Such a dissymmetric coordination reveals a significant stereochemical activity of the lone pair $6s^2$ electrons of Bi^{3+}, as is generally the case in Bi sulfosalts.

The six Cu positions are bound to four Se atoms. Cu1, Cu2, Cu4 and Cu6 have a quite regular tetrahedral coordination (Cu–Se from 2.42 to 2.56 Å), whereas Cu3 and Cu5 are closer to a planar triangular coordination (Cu–Se between 2.37 and 2.55 Å), with a fourth longer bond (2.885 and 2.915 Å). Minor Fe (with some Ni) detected with the electron-microprobe is probably incorporated as Fe^{3+} in tetrahedral Cu sites, as is generally the case in Cu–Fe chalcogenides, but it was not possible to locate it unequivocally, owing to the close *Z* values of Fe and Cu atoms. On the one hand, among the four tetrahedral Cu sites (nos. 1, 2, 4 and 6), Cu1 and Cu4, having a site-occupancy factor (s.o.f.) below 1 (Table 5), taking only Cu into account (0.968 and 0.979, respectively), are the most favorable to fix minor Fe, in order to adjust their s.o.f. closer to a full occupancy. On the other hand, according to Table 7, Cu2 and Cu6 correspond to the smallest tetrahedra, giving the highest bond-valence sums (1.26), in accordance of the incorporation of some Fe^{3+} (a smaller cation with a higher valence).

Short Cu–Cu distances are also present in the structure. The Cu5–Cu5 distance is 2.500 Å, forming a Cu–Cu–Cu zigzag chain along **a**. The Cu3–Cu6 distance is 2.656 Å, forming another Cu–Cu–Cu zigzag chain also along **a**. Atoms Cu1 and Cu2 form isolated Cu–Cu pairs with $d = 2.559$ Å, connected through a Cu1–Cu1–Cu1 zigzag chain along **a** with $d = 2.759$ Å. A similar zigzag chain, with $d = 2.634$ Å, is present along **b** in the crystal structure of $Cu_4Bi_4Se_7(Se_2)$ (Makovicky *et al.* 2002). All these distances are comparable to the Cu–Cu distance (2.555 Å) in 12-coordinated Cu metal. Such short distances do not correspond necessarily to direct Cu–Cu chemical bonding. In eldragónite, the Cu positions have relatively high isotropic displacement parameters, whereas their anisotropic displacement parameters are heterogeneous. These Cu positions are thus probably mean positions. In a well-resolved structure, it is possible that such short Cu–Cu distances would be excluded.

Building blocks

The projection along **a** of the crystal structure of eldragónite (Fig. 4) allows one to distinguish two slabs alternating along **b**. The thin slab A is a zigzag layer containing only Cu atoms within and Se atoms at the margin, with formula Cu_6Se_6. This layer is directly derived from the CaF_2 archetype. Figure 6 is the projection along $[\bar{1}01]$ of the CaF_2 structure, where only one such $(1\bar{1}1)$ zigzag layer has been selected. The layer results from the succession of $(100)_{CaF2}$ and $(111)_{CaF2}$ ribbons.

The thick slab B has Cu and Bi atoms at the margins, followed by Se mono-atomic layers, and a mixed (Cu_2Se) mono-atomic layer at the center, which gives the composition $(CuBi)_2(Se_2)_2(Cu_2Se)_2 = Cu_6Bi_2Se_6$. The whole formula is:

$$A + B = Cu_6Se_6 + Cu_6Bi_2Se_6 = Cu_{12}Bi_2Se_{12} = 2\,[Cu_6BiSe_4(Se_2)].$$

TABLE 5. SITE-OCCUPANCY FACTORS, FRACTIONAL COORDINATES (Å), AND EQUIVALENT ISOTROPIC-DISPLACEMENT PARAMETERS (Å²) OF ATOMS IN ELDRAGÓNITE

atom	s.o.f.	*x*	*y*	*z*	U_{eq}
Bi	1.00	0.25	0.614316(10)	0.10659(3)	0.01553(9)
Cu1	0.968(4)	0.25	0.02265(3)	0.07475(11)	0.0196(3)
Cu2	1.002(4)	0.25	0.11574(3)	0.02738(10)	0.0213(3)
Cu3	1.008(4)	0.25	0.78781(4)	0.19084(13)	0.0280(4)
Cu4	0.978(4)	0.25	0.55445(4)	0.78117(11)	0.0218(3)
Cu5	0.960(4)	0.25	0.50190(5)	0.07705(14)	0.0346(4)
Cu6	0.990(4)	0.25	0.26005(3)	0.14636(11)	0.0191(3)
Se1	1.00	0.25	0.39728(2)	0.13545(7)	0.01269(14)
Se2	1.00	0.25	0.56504(2)	0.52343(8)	0.01333(14)
Se3	1.00	0.25	0.17350(2)	0.21325(7)	0.01256(15)
Se4	1.00	0.25	0.03593(3)	0.33309(7)	0.01354(15)
Se5	1.00	0.25	0.33404(2)	0.31352(7)	0.01238(14)
Se6	1.00	0.25	0.76739(3)	0.49037(8)	0.01386(15)

TABLE 6. ANISOTROPIC DISPLACEMENT PARAMETERS OF THE ATOMS IN ELDRAGÓNITE

atom	U_{11}	U_{22}	U_{33}	U_{23}
Bi	0.01489(16)	0.01438(12)	0.01733(16)	0.00021(10)
Cu1	0.0221(5)	0.0141(5)	0.0228(6)	0.0003(4)
Cu2	0.0268(6)	0.0180(5)	0.0190(5)	-0.0029(4)
Cu3	0.0154(5)	0.0214(5)	0.0472(7)	-0.0097(5)
Cu4	0.0269(6)	0.0165(5)	0.0220(5)	0.0023(4)
Cu5	0.0130(5)	0.0559(9)	0.0347(7)	-0.0206(6)
Cu6	0.0175(5)	0.0175(5)	0.0222(5)	0.0010(4)
Se1	0.0136(3)	0.0120(3)	0.0124(3)	0.0003(2)
Se2	0.0111(3)	0.0118(3)	0.0171(3)	-0.0007(3)
Se3	0.0138(3)	0.0114(3)	0.0124(3)	0.0003(2)
Se4	0.0161(3)	0.0123(3)	0.0122(3)	0.0010(2)
Se5	0.0137(3)	0.0112(3)	0.0123(3)	0.0003(2)
Se6	0.0130(3)	0.0130(3)	0.0156(3)	-0.0016(2)

U_{13} and $U_{12} = 0$.

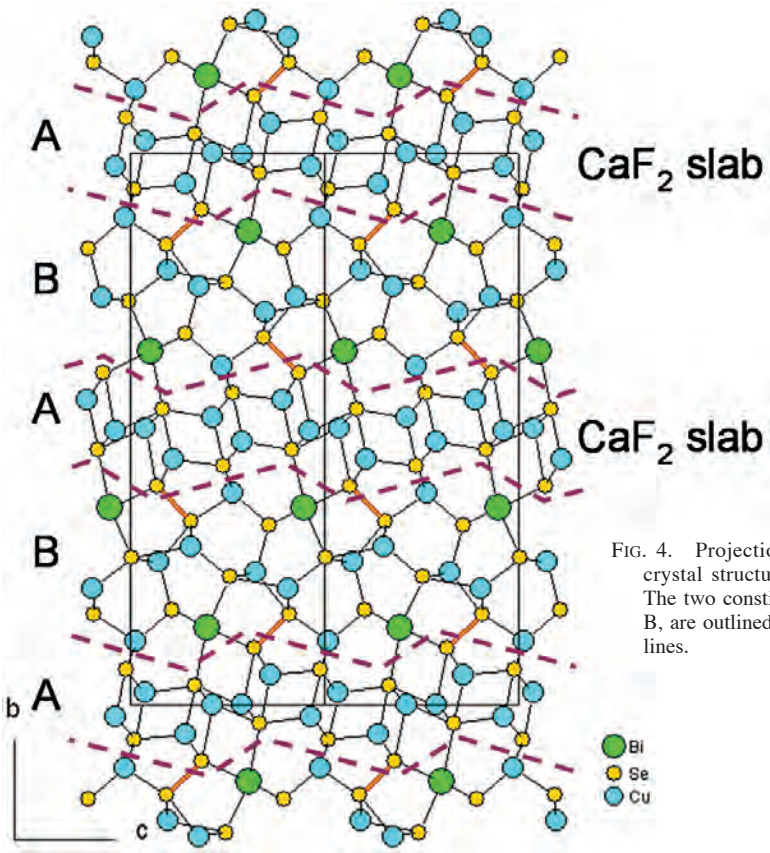

FIG. 4. Projection along **a** of the crystal structure of eldragónite. The two constituent slabs, A and B, are outlined by zigzag dashed lines.

TABLE 7. BOND DISTANCES AND BOND VALENCES IN THE CRYSTAL STRUCTURE OF ELDRAGÓNITE

	Bi1		Cu1		Cu2		Cu3		Cu4		Cu5		Cu6		Se1		Se5		Sum	
	d (Å)	b.v.	d (Å)	b.v.	d (Å)	b.v.	d (Å)	b.v.	d (Å)	b.v.	d (Å)	b.v.	d (Å)	b.v.	d (Å)	b.v.	d (Å)	b.v.	b.v.	
Se1	3.241	0.24							2.532	0.25	2.885	0.10					2.413	0.80	1.88	Se1
	3.241	0.24							2.532	0.25										
Se2			2.423	0.34	2.487	0.28			2.480	0.29									1.73	Se2
			2.503	0.27	2.487	0.28														
			2.503	0.27																
Se3	2.792	0.82			2.367	0.39							2.427	0.33					2.36	Se3
	2.792	0.82																		
Se4	3.539	0.11	2.495	0.28					2.495	0.28	2.378	0.38							1.78	Se4
	3.539	0.11									2.378	0.38								
											2.546	0.24								
Se5					2.454	0.31	2.374	0.38					2.561	0.23	2.41	0.80			2.10	Se5
							2.374	0.38												
Se6	2.709	1.03					2.429	0.33					2.411	0.35					2.15	Se6
							2.915	0.09					2.411	0.35						
Sum b.v.	Bi1	3.37	Cu1	1.16	Cu2	1.26	Cu3	1.18	Cu4	1.07	Cu5	1.10	Cu6	1.26			Sum cations	10.40	12.00	Sum Se

b.v.: bond valences calculated according to Brese & O'Keeffe (1991), without Fe or Ni at Cu positions.

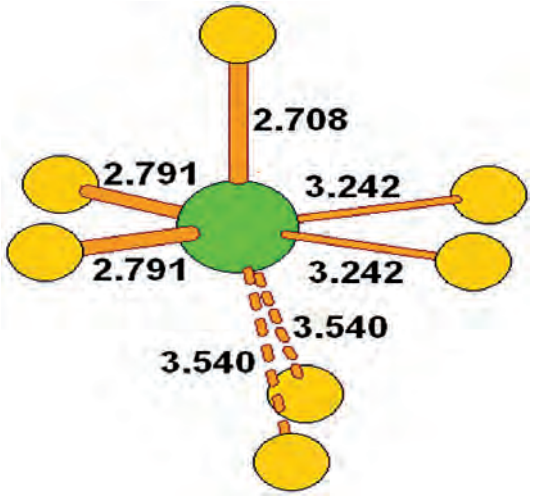

FIG. 5. Coordination of the Bi atom in the crystal structure of eldragónite.

The last formula takes into account the Se–Se pair at the junction between A and B slabs (Fig. 6).

Relationship with other chalcogenides

In its general organization, the crystal structure of eldragónite is quite original. The organization of the B layer is similar to, but distinct from, that of the constitutive layer of wittichenite, Cu_3BiS_3 (Kocman & Nuffield 1973). In schlemaite, $(Cu_{4.93}Ag_{0.40})(Pb_{0.61}Bi_{0.39})Se_4$ (Förster *et al.* 2003), there is also a ribbon of the $(100)_{CaF2}$ type within a zigzag layer parallel to (001) with parameters $a \times b = 9.5341 \times 4.1004$ Å, close to $c \times a = 9.559 \times 4.0341$ Å of eldragónite, but the two zigzag layers are not isotypic, and eldragónite cannot be considered as an expanded homologue of schlemaite.

Charge balance in eldragónite

The structural formula of eldragónite, ideally $Cu^{+}{}_6Bi^{3+}Se^{2-}{}_4(Se_2)^{2-}$, does not respect the valence equilibrium on the basis of integer oxidation states for cations and Se: there are nine positive charges for 10 negative ones, *i.e.*, a deficit of positive charges. On the other hand, with the electron-microprobe data, with minor Fe and Ni in the trivalent state,

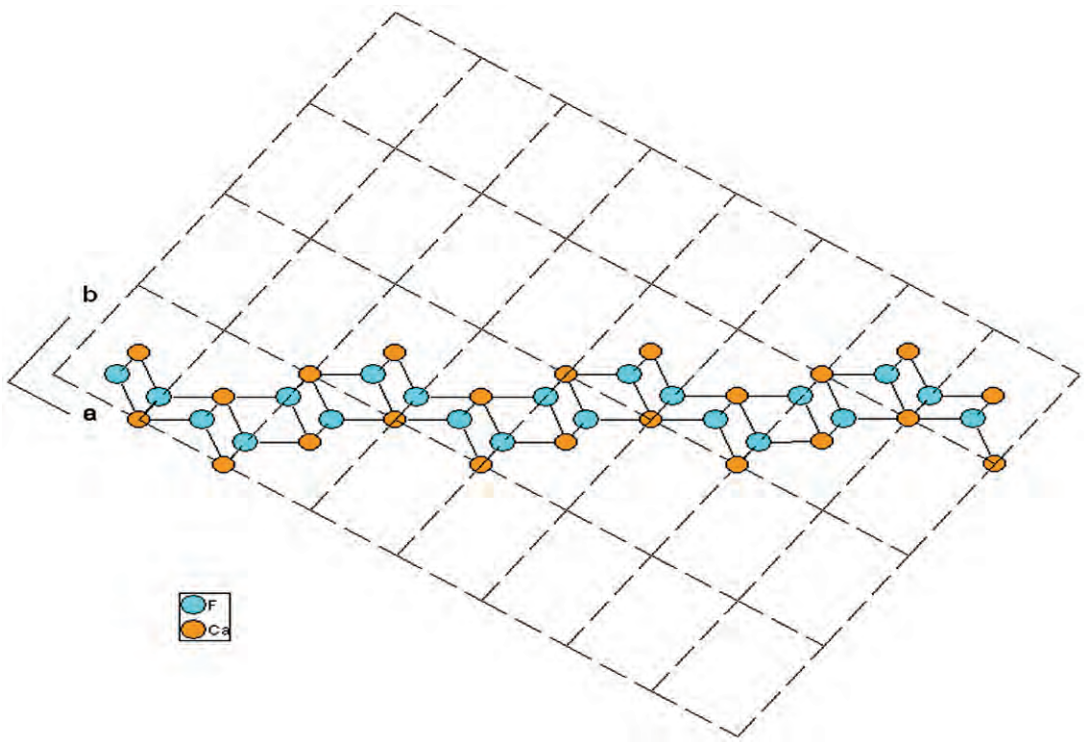

FIG. 6. Projection along [01] of the CaF_2 structure, with selection of a zigzag $(1\bar{2}1)$ slab corresponding to the A slab of the eldragónite structure.

$(Cu^{+}_{5.98}Fe^{3+}_{0.24}Ni^{3+}_{0.06})_{\Sigma 6.28}Bi^{3+}_{1.03}(Se_2)^{2-}Se^{2-}_{3.69}$, one has 9.97 positive charges for 9.38 negative ones, *i.e.*, an excess of positive charges. Such a discrepancy may be due to 1) the uncertainties of the crystal-structure refinement on a very small, composite sample, especially concerning the localization of minor Fe and Ni, and 2) the possibility of an artefact during the electron-microprobe analysis (decomposition of this Se-excess mineral under the electron beam), which would explain the Se deficit relative to the structural formula (which indicates no Se vacancy, nor a Cu interstitial atom).

Variations of bond valences calculated according to Brese & O'Keeffe (1991) illustrate the uncertainties of the crystal-structure solution. Table 7 indicates a large variation in the bond valence of the Se atoms, from 1.73 up to 2.36 *vu*; the same is evident from the valence of Cu atoms (invariably above 1: from 1.07 up to 1.26 *vu*), and the bond valence of Bi is overestimated (3.37 *vu*).

Discussion and Conclusions

In the vast group of sulfosalts and related minerals (Moëlo *et al.* 2008), eldragónite is a new example of the sparse subcategory of Se or (Se,S) derivatives, *i.e.*, selenio-(sulfo)salts, which contains about twenty mineral species (Table 8). Among all these minerals, eldragónite is the only one that presents a Se_2 pair within the structure, and thus corresponds to a mixed selenide–diselenide compound. A synthetic compound with similar crystal chemistry has been described by Makovicky *et al.* (2002); it also presents a Se_2 pair, with the formula $Cu_4Bi_4Se_7(Se_2)$, but its crystal structure is quite distinct. During an experimental study of the system Cu–Bi–Se between 300 and 750°C, Karup-Møller (2003) obtained the Se-rich phase "D", $Cu_3Bi_2Se_6$, at 300 and 350°C, but its structure is unknown; he did not observe a synthetic equivalent of eldragónite, which indicates that this mineral is probably stable only at a temperature below 300°. Three other Cu–Bi–Se synthetic compounds are known, $CuBiSe_2$, Cu_3BiSe_3 and $Cu_{1.78}Bi_{4.73}Se_8$ (Makovicky *et al.* 2006), and there is no unnamed mineral of this type (Smith & Nickel 2007). Eldragónite is thus the first natural Cu–Bi selenosalt.

Among unanswered questions, we must point to the uncertainties relative to the crystal-structure solution, especially the exact location of minor Fe and Ni. It is possible that these metals, probably in the trivalent state, are critical for the equilibrium of charges, and for the formation of eldragónite in nature. In this case, the true formula of eldragónite could be $[Cu_{5.5}(Fe,Ni)_{0.5}]BiSe_4(Se_2)$. But the absence of Fe and Ni in the eldragónite-type mineral from the San Francisco mine (Table 2) would contradict such a hypothesis. Only the study of homogeneous crystals of eldragónite will lead to a solution of this question.

The formation of eldragónite is conditioned by a high activity of Se, as indicated by the Se excess related to the Se_2 pair in its structure. Various selenides described at El Dragón illustrate such a Se excess relative to Cu and other transition metals: the krut'aite ($CuSe_2$) – penroseite ($NiSe_2$) – trogtalite ($CoSe_2$) series, klockmannite (CuSe) and umangite (Cu_3Se_2). According to the metallographic study of the ore association (see above), the formation of eldragónite is the geochemical result of a superimposition process, when a late hydrothermal stage, bringing the heavy metals (Bi, Pb and Hg) in solution as a result of a new tectonic phase, has reacted with pre-existing krut'aite. Dissolution of that diselenide provided the Se for the precipitation of heavy metals, generally combined with a residual fraction of Cu from krut'aite. This explains the formation of eldragónite together with rare and complex selenosalts in which Cu is combined with Pb, Bi and Hg.

TABLE 8. MINERALS OF THE SELENO-(SULFO-)SALT TYPE

Species	Formula	Main cations
Giraudite	$Cu_6[Cu_4(Fe,Zn)_2]As_4Se_{13}$	Cu,Fe/As
Chaméanite [1]	$(Cu,Fe)_4As(Se,S)_4$	Cu,Fe/As
Mgriite [1]	$(Cu,Fe)_3AsSe_3$	Cu,Fe/As
Permingeatite [2]	Cu_3SbSe_4	Cu/Sb
Hakite	$Cu_6[Cu_4Hg_2]Sb_4Se_{13}$	Cu,Hg/Sb
Eldragónite	$\mathbf{Cu_6BiSe_4(Se_2)}$	Cu/Bi
Selenopolybasite	$Cu(Ag,Cu)_6Ag_9Sb_2(S,Se)_9Se_2$	Ag,Cu/Sb
Selenostephanite	$Ag_5Sb(Se,S)_4$	Ag/Sb
Tsnigriite	$Ag_9Sb(S,Se)_3Te_3$	Ag/Sb
Bohdanowiczite	$AgBiSe_2$	Ag/Bi
Schlemaite [3]	$Cu_{6-x}(Pb_{1-x}Bi_x)Se_4$	Cu,Pb/Bi
Phase "A"	$\mathbf{Cu_5HgPb_2Bi_3Se_{10}}$	Cu,Hg,Pb/Bi
Petrovicite	$\mathbf{Cu_3HgPbBiSe_5}$	Cu,Hg,Pb/Bi
Phase "B"	$\mathbf{Cu_2HgPbBi_2Se_6}$	Cu,Hg,Pb/Bi
Součekite	$CuPbBi(S,Se)_3$	Cu,Pb/Bi
Watkinsonite	$\mathbf{Cu_2PbBi_4(Se,S)_8}$	Cu,Pb/Bi
Nordströmite	$CuPb_3Bi_7(S,Se)_{14}$	Pb,Cu/Bi
Junoite	$Cu_2Pb_3Bi_8(S,Se)_{16}$	Pb,Cu/Bi
Proudite	$Cu_2Pb_{16}Bi_{20}(S,Se)_{47}$	Pb,Cu/Bi
Weibullite	$Ag_{0.33}Pb_{5.33}Bi_{8.33}(S,Se)_{18}$	Pb,Ag/Bi
Wittite	$Pb_8Bi_{10}(S,Se)_{23}$	Pb/Bi
Babkinite	$Pb_2Bi_2(S,Se)_3$	Pb/Bi
Mozgovaite	$PbBi_4(S,Se)_7$	Pb/Bi
Crerarite	$(Pt,Pb)Bi_3(S,Se)_{4-x}$	Pt,Pb/Bi

[1] Probably the same species. [2] With Sb^{5+}. [3] Borderline compound (not exactly a sulfosalt). In bold, minerals present at El Dragón.

Acknowledgements

The authors dedicate this paper to Emil Makovicky, Professor at the University of Copenhagen, in honor of his outstanding research in the field of sulfosalts and their structures. On the occasion of a meeting of two of the authors (WHP and DT) with him during the poster session of the IMA conference in Toronto (1998), he immediately recognized the eminent importance of sulfosalt occurrences in the Austrian Alps, especially those of the tungsten mine at Felbertal, Salzburg, and

stimulated their investigation. This served as the starting point for several sulfosalt projects at the Institute of Mineralogy, Salzburg University. Emil has been closely associated with this research, and his valuable input has been key to the successful characterization of many new sulfosalts from Salzburg and abroad. We thank him for his insightful collaboration, treasure his friendship over the years, and wish him the best in his future endeavors with this exotic family of minerals.

We owe sincere thanks to Frank C. Hawthorne for the use of his diffractometer at the University of Manitoba. The authors are very grateful to Ricardo L. Sureda (University of Salta, Argentina) for having been an invaluable friend and excellent guide during several stays in the Bolivian Ag–Sn belt. We appreciate the financial support of several projects in the Porco area through the Austrian Academy of Sciences (ÖAW, Kommission für Grundlagen der Mineralrohstoffforschung), in particular Prof. Mining Engineer Dr. H. Wagner; this support allowed us to visit El Dragón. Georg Zagler (Salzburg) determined the VHN, Helmut Mühlhans (Leoben) prepared numerous high-quality polished sections and analyzed the mineral. The electron-microprobe facility at the University of Leoben is operated by the "Universitätszentrum Angewandte Geowissenschaften (UZAG)", a consortium of the Montanuniversität Leoben, the University of Graz and the Graz University of Technology. The authors acknowledge the supply of additional material from El Dragón by Prof. Hermann Wotruba, University of Aachen, Germany, and Mark Feinglos, Durham, North Carolina, USA. We express our sincere thanks to Milka K. de Brodtkorb, of the University of Buenos Aires, and María Florencia Márquez Zavalía (Mendoza, Argentina) for providing a polished section from the San Francisco mine, La Rioja, and to A. Martin-Izard (Oviedo, Spain) and H.J. Bernhardt (Bochum, Germany) for their electron-microprobe results. We appreciate very much the suggestions of Guest Editor Tonci Balić-Žunić, Nigel Cook and an anonymous reviewer, as well as the editorial care of Robert F. Martin, which all led to an improvement of the manuscript.

References

Ahlfeld, F. (1941): El yacimiento de selenio de Pacajake. *Ministerio de la Economia Nacional Boletin Informativo*, La Paz, Bolivia **1**(2), 23-28.

Ahlfeld, F. & Schneider-Scherbina, A. (1964): Los yacimientos minerales y de hidrocarburos de Bolivia. *Boletin de Departamento Nacional de Geología del Ministerio de Minas y Petroléo* **5** (Especiál), 1-388.

Amann, G., Paar, W.H., Robl, K. & Sureda, R.J. (1999): Late Cenozoic structural evolution of the western Sierras Pampeanas and selenium-mineralization of Sierra de Cacho area (Province of La Rioja, Argentina). EUG 10, Abstr. Vol. **4**(1), 416.

Block, H. & Ahlfeld, F. (1937): Die Selenerzlagerstätte Pacajake, Bolivia. *Z. prakt. Geol.* **45**, 9-14.

Brese, N.E. & O'Keeffe, M. (1991): Bond-valence for solids. *Acta Crystallogr.* **B47**, 192-197.

Brodtkorb, M.K. de & Crosta, S. (2010): Reseña de la ubicación geográfica de los seleniuros de la Sierra de Umango, provincia de La Rioja. *Revista de la Asociación Geológica Argentina* **67**(2), 272-277.

Brodtkorb, M.K. de, Gay, H.D. & Sureda, R.J. (1990): Carboniferous epithermal mineralizing thermal activity in the Precordilla. The polymetallic selenide–sulfide mineralization of Los Llantenes mining district, La Rioja, Argentina. *In* Proc. Eighth Int. Symp. Andean Geodynamics (Grenoble), Extended Abstr., 66-67.

Brodtkorb, M.K. de, Gay, H.D. & Sureda, R.J. (1993): Polymetallic selenide–sulfide minerals of the Los Llantenes mining district, La Rioja, Argentina. *Proc. 8th Quadrennial IAGOD Symp.* **1**, 119-125.

Förster, H.-J., Cooper, M.A., Roberts, A.C., Stanley, C.J., Hawthorne F.C., Laflamme, J.H.G. & Tischendorf, C. (2003): Schlemaite, $(Cu,\square)_6(Pb,Bi)Se_4$, a new mineral species from Niederschlema–Alberoda, Erzgebirge, Germany: description and crystal structure. *Can. Mineral.* **41**, 1433-1444.

Grundmann, G., Lehrberger, G. & Schnorrer-Köhler, G. (1990): The El Dragón mine, Potosi, Bolivia. *Mineral. Rec.* **21**, 133-146.

Guerrero, M.A. (1969): Informe del distrito minero Los Llantenes, depto. Sarmiento La Rioja. Serv. Min. Nac. Buenos Aires, Argentina. Unpubl. Rep.

Karup-Møller, S. (2003): The Cu–Bi–Se phase system at temperatures between 300°C and 750°C. *Neues Jahrb. Mineral., Monatsh.*, 556-576.

Keller, R., Holzapel, W.B. & Schulz, H. (1977): Effect of pressure on the atom positions in Se and Te. *Phys. Rec., Ser.* 3, B**16**, 4404-4412.

Kempff, O., Paar, W.H. & Tawackoli, S. (2009): *Minerales de Bolivia*. Comunicaciones El País SA. Zona Sur, La Paz, Bolivia.

Kempff, O., Tawackoli, S. & Paar, W.H. (2003): *Minerales de Bolivia*. SPC Impresores S.A., La Paz, Bolivia.

Kocman, V. & Nuffield, E.W. (1973): The crystal structure of wittichenite, Cu_3BiS_3. *Acta Crystallogr.* **B29**, 2528-2535.

Makovicky, E., Søtofte, I. & Karup-Møller, S. (2002): The crystal structure of $Cu_4Bi_4Se_9$. *Z. Kristallogr.* **217**, 597-604.

Makovicky, E., Søtofte, I. & Karup-Møller, S. (2006): The crystal structure of $Cu_{1.78}Bi_{4.73}Se_8$, a N = 3 pavonite homologue with a Cu-for-Bi substitution. *Z. Kristallogr.* **221**, 122-127.

Moëlo, Y., Makovicky, E., Mozgova, N.N., Jambor, J.L., Cook, N., Pring, A., Paar, W.H., Nickel, E.H., Graeser, S., Karup-Møller, S., Balić-Žunić, T., Mumme, W.G., Vurro, F., Topa, D., Bindi, L., Bente, K. & Shimizu, M. (2008): Sulfosalt systematics: a review. Report of the sulfosalt sub-committee of the IMA Commission on Ore Mineralogy. *Eur. J. Mineral.* **20**, 7-46.

Paar, W.H., Amann, G., Sureda, R.J. & Brodtkorb, M.K. de (2002a): Selenium mineralization associated with precious metals in the Sierra de Umango, Argentina. *Eighteenth Gen. Meeting, Int. Mineral. Assoc.* (*Edinburgh*), *Abstr.*, 265-266.

Paar, W.H., Amann, G., Topa, D. & Sureda, R.J. (2000): Gold and palladium in the Sierra de Umango and Los Llantenes selenide districts, La Rioja, Argentina. *Mem. XIV Congreso Geologico Boliviano* (*La Paz*), 465-469.

Paar, W.H., Brodtkorb, M.K. de & Sureda, R.J. (2004d): Palladium, platinum, gold and silver in selenide districts of NW-Argentina. *Thirty-second Int. Geol. Conf.* (*Florence*), *Abstr.* (part 1), 277.

Paar, W.H., Roberts, A.C., Criddle, A.J. & Topa, D. (1998a): A new mineral, chrisstanleyite, $Ag_2Pd_3Se_4$, from Hope's Nose, Torquay, Devon, England. *Mineral. Mag.* **62**, 257-264.

Paar, W.H., Sureda, R.J. & Brodtkorb, M.K. de (1996a): Mineralogía de los yacimientos de selenio en La Rioja, Argentina. Krutaita, tyrrellita y trogtalita de Los Llantenes. *Rev. Asociación Geológica Argentina* **51**, 304-312.

Paar, W.H., Sureda, R.J. & Brodtkorb, M.K. de (1996b): Oro y plata en los yacimientos de selenio de La Rioja, Argentina: hallazgo de fischesserita, Ag_3AuSe_2. *III Reunion de Mineralogía y Metalogenia. Publicación del Instituto de Recursos Minerales. Univ. Nac. de la Plata* **5**, 177-185.

Paar, W.H., Sureda, R.J. & Topa, D. (2004b): Chrisstanleyita, $Ag_2Pd_3Se_4$, y su analogo cuprífero jagüéita, $Cu_2Pd_3Se_4$, de la mina El Chire, Departamento Gral. Lamadrid, Provincia de La Rioja, Argentina. 7° Congreso de Mineralogía y Metalogenía, Artículo, 109-112.

Paar, W.H., Sureda, R.J., Topa, D. & Amann, G. (1998b): New data on the selenide district of the Sierra de Umango, Province of La Rioja, Argentina. Geowissenschaftl. Lateinamerika-Kolloquium (Bayreuth). *Terra Nostra* **98**(5), 117.

Paar, W.H., Topa, D., Makovicky, E., Sureda, R.J., Brodtkorb, M.K. de, Nickel, E.H. & Putz, H. (2004a): Jagüéite, $Cu_2Pd_3Se_4$, a new mineral species from El Chire, La Rioja, Argentina. *Can. Mineral.* **42**, 1745-1755.

Paar, W.H., Topa, D., Roberts, A.C., Criddle, A.J., Amann, G. & Sureda, R.J. (2002b): The new mineral species brodtkorbite, Cu_2HgSe_2, and the associated selenide assemblage from Tuminico, Sierra de Cacho, La Rioja, Argentina. *Can. Mineral.* **40**, 225-237.

Paar, W.H., Topa, D., Sureda, R.J., Stumpfl, E.F. & Mühlhans, H. (2004c): Merenskyita, $PdTe_2$, en las menas de selenio, cobre y plata de la mina Las Asperezas, Distrito Minero Sierra de Umango, Provincia de La Rioja, Argentina.- 7% Congreso Mineralogía y Metalogenía, Artículo, 113-118.

Redwood, S.D. (2003): The Pacajake selenium mine, Potosi, Bolivia. *Mineral. Rec.* **34**, 339-357.

Sheldrick, G.M. (1997): *Program for the Solution and Refinement of Crystal Structures*. University of Göttingen, Göttingen, Germany.

Smith, D.G.W. & Nickel, E.H. (2007): A system for codification for unnamed minerals: report of the Subcommittee for Unnamed Minerals of the IMA Commission on New Minerals, Nomenclature and Classification. *Can. Mineral.* **45**, 983-1055.

Topa, D., Makovicky, E., Sejkora, J. & Dittrich, H. (2010): The crystal structure of watkinsonite, $Cu_2PbBi_4(Se,S)_8$, from the Zálesi uranium deposit, Czech Republic. *Can. Mineral.* **48**, 1109-1118.

Young, B.B. & Millman, A.P. (1964): Microhardness and deformation characteristics of ore minerals. *Inst. Mining Metall. Trans.* **73**, 437-466.

Received May 18, 2011, revised manuscript accepted March 7, 2012.

```
data_cubise

_audit_creation_method            SHELXL-97
_chemical_name_systematic
;
 ?
;
_chemical_name_common             ?
_chemical_melting_point           ?
_chemical_formula_moiety          ?
_chemical_formula_sum
 'Bi Cu6 Se6'
_chemical_formula_weight          1063.98

loop_
 _atom_type_symbol
 _atom_type_description
 _atom_type_scat_dispersion_real
 _atom_type_scat_dispersion_imag
 _atom_type_scat_source
 'Cu'  'Cu'   0.3201   1.2651
 'International Tables Vol C Tables 4.2.6.8 and 6.1.1.4'
 'Se'  'Se'  -0.0929   2.2259
 'International Tables Vol C Tables 4.2.6.8 and 6.1.1.4'
 'Bi'  'Bi'  -4.1077  10.2566
 'International Tables Vol C Tables 4.2.6.8 and 6.1.1.4'

_symmetry_cell_setting            ?
_symmetry_space_group_name_H-M    ?

loop_
 _symmetry_equiv_pos_as_xyz
 'x, y, z'
 '-x, y+1/2, -z+1/2'
 'x+1/2, -y, -z'
 '-x+1/2, -y+1/2, z+1/2'
 '-x, -y, -z'
 'x, -y-1/2, z-1/2'
 '-x-1/2, y, z'
 'x-1/2, y-1/2, -z-1/2'

_cell_length_a                    4.0341(4)
_cell_length_b                    27.056(3)
_cell_length_c                    9.5559(9)
_cell_angle_alpha                 90.00
_cell_angle_beta                  90.00
_cell_angle_gamma                 90.00
_cell_volume                      1042.99(18)
_cell_formula_units_Z             4
_cell_measurement_temperature     293(2)
_cell_measurement_reflns_used     ?
_cell_measurement_theta_min       ?
_cell_measurement_theta_max       ?
```

```
_exptl_crystal_description        ?
_exptl_crystal_colour             ?
_exptl_crystal_size_max           ?
_exptl_crystal_size_mid           ?
_exptl_crystal_size_min           ?
_exptl_crystal_density_meas       ?
_exptl_crystal_density_diffrn     6.776
_exptl_crystal_density_method     'not measured'
_exptl_crystal_F_000              1844
_exptl_absorpt_coefficient_mu     49.680
_exptl_absorpt_correction_type    ?
_exptl_absorpt_correction_T_min   ?
_exptl_absorpt_correction_T_max   ?
_exptl_absorpt_process_details    ?

_exptl_special_details
;
 ?
;

_diffrn_ambient_temperature       293(2)
_diffrn_radiation_wavelength      0.71073
_diffrn_radiation_type            MoK\a
_diffrn_radiation_source          'fine-focus sealed tube'
_diffrn_radiation_monochromator   graphite
_diffrn_measurement_device_type   ?
_diffrn_measurement_method        ?
_diffrn_detector_area_resol_mean  ?
_diffrn_standards_number          ?
_diffrn_standards_interval_count  ?
_diffrn_standards_interval_time   ?
_diffrn_standards_decay_%         ?
_diffrn_reflns_number             1731
_diffrn_reflns_av_R_equivalents   0.0000
_diffrn_reflns_av_sigmaI/netI     0.0184
_diffrn_reflns_limit_h_min        0
_diffrn_reflns_limit_h_max        5
_diffrn_reflns_limit_k_min        0
_diffrn_reflns_limit_k_max        38
_diffrn_reflns_limit_l_min        0
_diffrn_reflns_limit_l_max        13
_diffrn_reflns_theta_min          1.51
_diffrn_reflns_theta_max          30.00
_reflns_number_total              1731
_reflns_number_gt                 1569
_reflns_threshold_expression      >2sigma(I)

_computing_data_collection        ?
_computing_cell_refinement        ?
_computing_data_reduction         ?
_computing_structure_solution     'SHELXS-97 (Sheldrick, 1990)'
_computing_structure_refinement   'SHELXL-97 (Sheldrick, 1997)'
_computing_molecular_graphics     ?
_computing_publication_material   ?
```

```
_refine_special_details
;
 Refinement of F^2^ against ALL reflections.  The weighted R-factor wR and
 goodness of fit S are based on F^2^, conventional R-factors R are based
 on F, with F set to zero for negative F^2^. The threshold expression of
 F^2^ > 2sigma(F^2^) is used only for calculating R-factors(gt) etc. and is
 not relevant to the choice of reflections for refinement.  R-factors based
 on F^2^ are statistically about twice as large as those based on F, and R-
 factors based on ALL data will be even larger.
;

_refine_ls_structure_factor_coef  Fsqd
_refine_ls_matrix_type            full
_refine_ls_weighting_scheme       calc
_refine_ls_weighting_details
 'calc w=1/[\s^2^(Fo^2^)+(0.0175P)^2^+5.9199P] where P=(Fo^2^+2Fc^2^)/3'
_atom_sites_solution_primary      direct
_atom_sites_solution_secondary    difmap
_atom_sites_solution_hydrogens    geom
_refine_ls_hydrogen_treatment     mixed
_refine_ls_extinction_method      none
_refine_ls_extinction_coef        ?
_refine_ls_number_reflns          1731
_refine_ls_number_parameters      86
_refine_ls_number_restraints      0
_refine_ls_R_factor_all           0.0320
_refine_ls_R_factor_gt            0.0263
_refine_ls_wR_factor_ref          0.0517
_refine_ls_wR_factor_gt           0.0496
_refine_ls_goodness_of_fit_ref    1.213
_refine_ls_restrained_S_all       1.213
_refine_ls_shift/su_max           0.001
_refine_ls_shift/su_mean          0.000

loop_
 _atom_site_label
 _atom_site_type_symbol
 _atom_site_fract_x
 _atom_site_fract_y
 _atom_site_fract_z
 _atom_site_U_iso_or_equiv
 _atom_site_adp_type
 _atom_site_occupancy
 _atom_site_symmetry_multiplicity
 _atom_site_calc_flag
 _atom_site_refinement_flags
 _atom_site_disorder_assembly
 _atom_site_disorder_group
Bi Bi 0.2500 0.641316(10) 0.10659(3) 0.01553(9) Uani 1 2 d S . .
Se1 Se 0.2500 0.39728(2) 0.13545(7) 0.01269(14) Uani 1 2 d S . .
Se2 Se 0.2500 0.56504(2) 0.52343(8) 0.01333(14) Uani 1 2 d S . .
Se3 Se 0.2500 0.17350(2) 0.21325(7) 0.01256(15) Uani 1 2 d S . .
Se4 Se 0.2500 0.03593(3) 0.33309(7) 0.01354(15) Uani 1 2 d S . .
Se5 Se 0.2500 0.33404(2) 0.31352(7) 0.01238(14) Uani 1 2 d S . .
Se6 Se 0.2500 0.76739(3) 0.49037(8) 0.01386(15) Uani 1 2 d S . .
```

```
Cu1 Cu 0.2500 0.02265(3) 0.07475(11) 0.0196(3) Uani 0.968(4) 2 d SP . .
Cu2 Cu 0.2500 0.11574(3) 0.02738(10) 0.0213(3) Uani 1.003(4) 2 d SP . .
Cu3 Cu 0.2500 0.78781(4) 0.19084(13) 0.0280(4) Uani 1.008(5) 2 d SP . .
Cu4 Cu 0.2500 0.55445(4) 0.78117(11) 0.0218(3) Uani 0.979(4) 2 d SP . .
Cu5 Cu 0.2500 0.50190(5) 0.07705(14) 0.0346(4) Uani 0.960(5) 2 d SP . .
Cu6 Cu 0.2500 0.26005(3) 0.14636(11) 0.0191(3) Uani 0.991(4) 2 d SP . .

loop_
 _atom_site_aniso_label
 _atom_site_aniso_U_11
 _atom_site_aniso_U_22
 _atom_site_aniso_U_33
 _atom_site_aniso_U_23
 _atom_site_aniso_U_13
 _atom_site_aniso_U_12
Bi 0.01489(16) 0.01438(12) 0.01733(16) 0.00021(10) 0.000 0.000
Se1 0.0136(3) 0.0120(3) 0.0124(3) 0.0003(2) 0.000 0.000
Se2 0.0111(3) 0.0118(3) 0.0171(3) -0.0007(3) 0.000 0.000
Se3 0.0138(3) 0.0114(3) 0.0124(3) 0.0003(2) 0.000 0.000
Se4 0.0161(3) 0.0123(3) 0.0122(3) 0.0010(2) 0.000 0.000
Se5 0.0137(3) 0.0112(3) 0.0123(3) 0.0003(2) 0.000 0.000
Se6 0.0130(3) 0.0130(3) 0.0156(3) -0.0016(2) 0.000 0.000
Cu1 0.0221(5) 0.0141(5) 0.0228(6) 0.0003(4) 0.000 0.000
Cu2 0.0268(6) 0.0180(5) 0.0190(5) -0.0029(4) 0.000 0.000
Cu3 0.0154(5) 0.0214(5) 0.0472(7) -0.0097(5) 0.000 0.000
Cu4 0.0269(6) 0.0165(5) 0.0220(5) 0.0023(4) 0.000 0.000
Cu5 0.0130(5) 0.0559(9) 0.0347(7) -0.0206(6) 0.000 0.000
Cu6 0.0175(5) 0.0175(5) 0.0222(5) 0.0010(4) 0.000 0.000

_geom_special_details
;
 All esds (except the esd in the dihedral angle between two l.s. planes)
 are estimated using the full covariance matrix.  The cell esds are taken
 into account individually in the estimation of esds in distances, angles
 and torsion angles; correlations between esds in cell parameters are only
 used when they are defined by crystal symmetry.  An approximate (isotropic)
 treatment of cell esds is used for estimating esds involving l.s. planes.
;

loop_
 _geom_bond_atom_site_label_1
 _geom_bond_atom_site_label_2
 _geom_bond_distance
 _geom_bond_site_symmetry_2
 _geom_bond_publ_flag
Bi Se6 2.7084(8) 6_575 ?
Bi Se3 2.7912(5) 2_655 ?
Bi Se3 2.7912(5) 2 ?
Bi Se1 3.2417(6) 5_565 ?
Bi Se1 3.2417(6) 5_665 ?
Se1 Se5 2.4132(10) . ?
Se1 Cu4 2.5316(7) 5_666 ?
Se1 Cu4 2.5316(7) 5_566 ?
Se1 Cu5 2.8849(17) . ?
Se1 Bi 3.2417(6) 5_565 ?
```

```
Se1 Bi 3.2417(6) 5_665 ?
Se2 Cu1 2.4225(12) 6_566 ?
Se2 Cu4 2.4796(13) . ?
Se2 Cu2 2.4872(7) 2_655 ?
Se2 Cu2 2.4872(7) 2 ?
Se2 Cu1 2.5028(7) 2 ?
Se2 Cu1 2.5028(7) 2_655 ?
Se3 Cu2 2.3659(12) . ?
Se3 Cu6 2.4273(12) . ?
Se3 Bi 2.7912(5) 2_645 ?
Se3 Bi 2.7912(5) 2_545 ?
Se4 Cu5 2.3778(8) 2_645 ?
Se4 Cu5 2.3778(8) 2_545 ?
Se4 Cu1 2.4948(13) . ?
Se4 Cu4 2.4951(12) 6_565 ?
Se4 Cu5 2.5460(14) 6_566 ?
Se5 Cu3 2.3738(7) 2_545 ?
Se5 Cu3 2.3738(7) 2_645 ?
Se5 Cu2 2.4542(12) 6_566 ?
Se5 Cu6 2.5611(12) . ?
Se6 Cu6 2.4114(7) 2 ?
Se6 Cu6 2.4114(7) 2_655 ?
Se6 Cu3 2.4289(13) 6_576 ?
Se6 Bi 2.7084(8) 6_576 ?
Se6 Cu3 2.9151(15) . ?
Cu1 Se2 2.4225(12) 6_565 ?
Cu1 Se2 2.5028(7) 2_645 ?
Cu1 Se2 2.5028(7) 2_545 ?
Cu1 Cu2 2.5590(14) . ?
Cu1 Cu1 2.7588(14) 5 ?
Cu1 Cu1 2.7588(14) 5_655 ?
Cu1 Cu4 2.8708(14) 6_565 ?
Cu2 Se5 2.4542(12) 6_565 ?
Cu2 Se2 2.4872(7) 2_545 ?
Cu2 Se2 2.4872(7) 2_645 ?
Cu3 Se5 2.3738(7) 2_655 ?
Cu3 Se5 2.3738(7) 2 ?
Cu3 Se6 2.4289(13) 6_575 ?
Cu3 Cu6 2.6557(11) 2_655 ?
Cu3 Cu6 2.6557(11) 2 ?
Cu4 Se4 2.4951(12) 6_566 ?
Cu4 Se1 2.5316(7) 5_666 ?
Cu4 Se1 2.5316(7) 5_566 ?
Cu4 Cu5 2.8684(13) 5_566 ?
Cu4 Cu5 2.8684(13) 5_666 ?
Cu4 Cu1 2.8708(14) 6_566 ?
Cu5 Se4 2.3778(8) 2_655 ?
Cu5 Se4 2.3778(8) 2 ?
Cu5 Cu5 2.4995(16) 5_565 ?
Cu5 Cu5 2.4995(16) 5_665 ?
Cu5 Se4 2.5460(14) 6_565 ?
Cu5 Cu4 2.8684(13) 5_566 ?
Cu5 Cu4 2.8684(13) 5_666 ?
Cu6 Se6 2.4114(7) 2_545 ?
Cu6 Se6 2.4114(7) 2_645 ?
```

```
Cu6 Cu3 2.6557(11) 2_645 ?
Cu6 Cu3 2.6557(11) 2_545 ?

loop_
 _geom_angle_atom_site_label_1
 _geom_angle_atom_site_label_2
 _geom_angle_atom_site_label_3
 _geom_angle
 _geom_angle_site_symmetry_1
 _geom_angle_site_symmetry_3
 _geom_angle_publ_flag
Se6 Bi Se3 88.187(19) 6_575 2_655 ?
Se6 Bi Se3 88.187(19) 6_575 2 ?
Se3 Bi Se3 92.55(2) 2_655 2 ?
Se6 Bi Se1 90.071(19) 6_575 5_565 ?
Se3 Bi Se1 171.985(15) 2_655 5_565 ?
Se3 Bi Se1 95.217(15) 2 5_565 ?
Se6 Bi Se1 90.071(19) 6_575 5_665 ?
Se3 Bi Se1 95.217(15) 2_655 5_665 ?
Se3 Bi Se1 171.985(15) 2 5_665 ?
Se1 Bi Se1 76.958(18) 5_565 5_665 ?
Se5 Se1 Cu4 98.27(3) . 5_666 ?
Se5 Se1 Cu4 98.27(3) . 5_566 ?
Cu4 Se1 Cu4 105.64(4) 5_666 5_566 ?
Se5 Se1 Cu5 146.31(4) . . ?
Cu4 Se1 Cu5 63.56(3) 5_666 . ?
Cu4 Se1 Cu5 63.56(3) 5_566 . ?
Se5 Se1 Bi 105.94(2) . 5_565 ?
Cu4 Se1 Bi 152.44(3) 5_666 5_565 ?
Cu4 Se1 Bi 83.97(2) 5_566 5_565 ?
Cu5 Se1 Bi 100.26(3) . 5_565 ?
Se5 Se1 Bi 105.94(2) . 5_665 ?
Cu4 Se1 Bi 83.97(2) 5_666 5_665 ?
Cu4 Se1 Bi 152.44(3) 5_566 5_665 ?
Cu5 Se1 Bi 100.26(3) . 5_665 ?
Bi Se1 Bi 76.958(18) 5_565 5_665 ?
Cu1 Se2 Cu4 71.69(4) 6_566 . ?
Cu1 Se2 Cu2 125.43(2) 6_566 2_655 ?
Cu4 Se2 Cu2 104.93(3) . 2_655 ?
Cu1 Se2 Cu2 125.43(2) 6_566 2 ?
Cu4 Se2 Cu2 104.93(3) . 2 ?
Cu2 Se2 Cu2 108.38(4) 2_655 2 ?
Cu1 Se2 Cu1 68.11(3) 6_566 2 ?
Cu4 Se2 Cu1 108.63(3) . 2 ?
Cu2 Se2 Cu1 146.42(4) 2_655 2 ?
Cu2 Se2 Cu1 61.70(3) 2 2 ?
Cu1 Se2 Cu1 68.11(3) 6_566 2_655 ?
Cu4 Se2 Cu1 108.63(3) . 2_655 ?
Cu2 Se2 Cu1 61.70(3) 2_655 2_655 ?
Cu2 Se2 Cu1 146.42(4) 2 2_655 ?
Cu1 Se2 Cu1 107.40(4) 2 2_655 ?
Cu2 Se3 Cu6 116.08(4) . . ?
Cu2 Se3 Bi 104.89(3) . 2_645 ?
Cu6 Se3 Bi 117.61(2) . 2_645 ?
Cu2 Se3 Bi 104.89(3) . 2_545 ?
```

```
Cu6 Se3 Bi 117.61(2) . 2_545 ?
Bi Se3 Bi 92.55(2) 2_645 2_545 ?
Cu5 Se4 Cu5 116.05(6) 2_645 2_545 ?
Cu5 Se4 Cu1 107.55(4) 2_645 . ?
Cu5 Se4 Cu1 107.55(4) 2_545 . ?
Cu5 Se4 Cu4 72.07(4) 2_645 6_565 ?
Cu5 Se4 Cu4 72.07(4) 2_545 6_565 ?
Cu1 Se4 Cu4 70.24(4) . 6_565 ?
Cu5 Se4 Cu5 60.90(3) 2_645 6_566 ?
Cu5 Se4 Cu5 60.90(3) 2_545 6_566 ?
Cu1 Se4 Cu5 148.01(5) . 6_566 ?
Cu4 Se4 Cu5 77.77(5) 6_565 6_566 ?
Cu3 Se5 Cu3 116.36(5) 2_545 2_645 ?
Cu3 Se5 Se1 111.18(3) 2_545 . ?
Cu3 Se5 Se1 111.18(3) 2_645 . ?
Cu3 Se5 Cu2 107.84(4) 2_545 6_566 ?
Cu3 Se5 Cu2 107.84(4) 2_645 6_566 ?
Se1 Se5 Cu2 101.22(4) . 6_566 ?
Cu3 Se5 Cu6 64.99(3) 2_545 . ?
Cu3 Se5 Cu6 64.99(3) 2_645 . ?
Se1 Se5 Cu6 96.57(4) . . ?
Cu2 Se5 Cu6 162.21(4) 6_566 . ?
Cu6 Se6 Cu6 113.54(5) 2 2_655 ?
Cu6 Se6 Cu3 112.13(3) 2 6_576 ?
Cu6 Se6 Cu3 112.13(3) 2_655 6_576 ?
Cu6 Se6 Bi 107.29(3) 2 6_576 ?
Cu6 Se6 Bi 107.29(3) 2_655 6_576 ?
Cu3 Se6 Bi 103.73(4) 6_576 6_576 ?
Cu6 Se6 Cu3 58.91(3) 2 . ?
Cu6 Se6 Cu3 58.91(3) 2_655 . ?
Cu3 Se6 Cu3 152.99(4) 6_576 . ?
Bi Se6 Cu3 103.28(3) 6_576 . ?
Se2 Cu1 Se4 109.96(4) 6_565 . ?
Se2 Cu1 Se2 111.89(3) 6_565 2_645 ?
Se4 Cu1 Se2 107.75(3) . 2_645 ?
Se2 Cu1 Se2 111.89(3) 6_565 2_545 ?
Se4 Cu1 Se2 107.75(3) . 2_545 ?
Se2 Cu1 Se2 107.40(4) 2_645 2_545 ?
Se2 Cu1 Cu2 158.13(5) 6_565 . ?
Se4 Cu1 Cu2 91.90(4) . . ?
Se2 Cu1 Cu2 58.85(2) 2_645 . ?
Se2 Cu1 Cu2 58.85(2) 2_545 . ?
Se2 Cu1 Cu1 57.33(3) 6_565 5 ?
Se4 Cu1 Cu1 125.20(4) . 5 ?
Se2 Cu1 Cu1 126.78(6) 2_645 5 ?
Se2 Cu1 Cu1 54.56(3) 2_545 5 ?
Cu2 Cu1 Cu1 110.22(5) . 5 ?
Se2 Cu1 Cu1 57.33(3) 6_565 5_655 ?
Se4 Cu1 Cu1 125.20(4) . 5_655 ?
Se2 Cu1 Cu1 54.56(3) 2_645 5_655 ?
Se2 Cu1 Cu1 126.78(6) 2_545 5_655 ?
Cu2 Cu1 Cu1 110.22(5) . 5_655 ?
Cu1 Cu1 Cu1 93.96(6) 5 5_655 ?
Se2 Cu1 Cu4 55.08(3) 6_565 6_565 ?
Se4 Cu1 Cu4 54.88(3) . 6_565 ?
```

```
Se2 Cu1 Cu4 126.19(2) 2_645 6_565 ?
Se2 Cu1 Cu4 126.19(2) 2_545 6_565 ?
Cu2 Cu1 Cu4 146.78(5) . 6_565 ?
Cu1 Cu1 Cu4 91.90(4) 5 6_565 ?
Cu1 Cu1 Cu4 91.90(4) 5_655 6_565 ?
Se3 Cu2 Se5 105.03(4) . 6_565 ?
Se3 Cu2 Se2 120.73(3) . 2_545 ?
Se5 Cu2 Se2 98.21(3) 6_565 2_545 ?
Se3 Cu2 Se2 120.73(3) . 2_645 ?
Se5 Cu2 Se2 98.21(3) 6_565 2_645 ?
Se2 Cu2 Se2 108.38(4) 2_545 2_645 ?
Se3 Cu2 Cu1 121.16(5) . . ?
Se5 Cu2 Cu1 133.81(5) 6_565 . ?
Se2 Cu2 Cu1 59.45(2) 2_545 . ?
Se2 Cu2 Cu1 59.45(2) 2_645 . ?
Se5 Cu3 Se5 116.36(5) 2_655 2 ?
Se5 Cu3 Se6 108.07(4) 2_655 6_575 ?
Se5 Cu3 Se6 108.07(4) 2 6_575 ?
Se5 Cu3 Cu6 60.92(3) 2_655 2_655 ?
Se5 Cu3 Cu6 143.58(6) 2 2_655 ?
Se6 Cu3 Cu6 106.75(4) 6_575 2_655 ?
Se5 Cu3 Cu6 143.58(6) 2_655 2 ?
Se5 Cu3 Cu6 60.92(3) 2 2 ?
Se6 Cu3 Cu6 106.75(4) 6_575 2 ?
Cu6 Cu3 Cu6 98.84(5) 2_655 2 ?
Se5 Cu3 Se6 96.73(4) 2_655 . ?
Se5 Cu3 Se6 96.73(4) 2 . ?
Se6 Cu3 Se6 131.14(4) 6_575 . ?
Cu6 Cu3 Se6 51.04(3) 2_655 . ?
Cu6 Cu3 Se6 51.04(3) 2 . ?
Se2 Cu4 Se4 108.11(4) . 6_566 ?
Se2 Cu4 Se1 104.66(3) . 5_666 ?
Se4 Cu4 Se1 116.30(3) 6_566 5_666 ?
Se2 Cu4 Se1 104.66(3) . 5_566 ?
Se4 Cu4 Se1 116.30(3) 6_566 5_566 ?
Se1 Cu4 Se1 105.64(4) 5_666 5_566 ?
Se2 Cu4 Cu5 122.04(4) . 5_566 ?
Se4 Cu4 Cu5 52.07(3) 6_566 5_566 ?
Se1 Cu4 Cu5 133.30(5) 5_666 5_566 ?
Se1 Cu4 Cu5 64.23(3) 5_566 5_566 ?
Se2 Cu4 Cu5 122.04(4) . 5_666 ?
Se4 Cu4 Cu5 52.07(3) 6_566 5_666 ?
Se1 Cu4 Cu5 64.23(3) 5_666 5_666 ?
Se1 Cu4 Cu5 133.30(5) 5_566 5_666 ?
Cu5 Cu4 Cu5 89.37(5) 5_566 5_666 ?
Se2 Cu4 Cu1 53.23(3) . 6_566 ?
Se4 Cu4 Cu1 54.87(3) 6_566 6_566 ?
Se1 Cu4 Cu1 126.23(2) 5_666 6_566 ?
Se1 Cu4 Cu1 126.23(2) 5_566 6_566 ?
Cu5 Cu4 Cu1 86.47(4) 5_566 6_566 ?
Cu5 Cu4 Cu1 86.47(4) 5_666 6_566 ?
Se4 Cu5 Se4 116.05(6) 2_655 2 ?
Se4 Cu5 Cu5 155.95(11) 2_655 5_565 ?
Se4 Cu5 Cu5 62.88(3) 2 5_565 ?
Se4 Cu5 Cu5 62.88(3) 2_655 5_665 ?
```

```
Se4 Cu5 Cu5 155.95(11) 2 5_665 ?
Cu5 Cu5 Cu5 107.60(10) 5_565 5_665 ?
Se4 Cu5 Se4 119.10(3) 2_655 6_565 ?
Se4 Cu5 Se4 119.10(3) 2 6_565 ?
Cu5 Cu5 Se4 56.22(5) 5_565 6_565 ?
Cu5 Cu5 Se4 56.22(5) 5_665 6_565 ?
Se4 Cu5 Cu4 129.18(6) 2_655 5_566 ?
Se4 Cu5 Cu4 55.86(3) 2 5_566 ?
Cu5 Cu5 Cu4 71.88(5) 5_565 5_566 ?
Cu5 Cu5 Cu4 145.48(9) 5_665 5_566 ?
Se4 Cu5 Cu4 102.64(4) 6_565 5_566 ?
Se4 Cu5 Cu4 55.86(3) 2_655 5_666 ?
Se4 Cu5 Cu4 129.18(6) 2 5_666 ?
Cu5 Cu5 Cu4 145.48(9) 5_565 5_666 ?
Cu5 Cu5 Cu4 71.88(5) 5_665 5_666 ?
Se4 Cu5 Cu4 102.64(4) 6_565 5_666 ?
Cu4 Cu5 Cu4 89.37(5) 5_566 5_666 ?
Se4 Cu5 Se1 108.07(4) 2_655 . ?
Se4 Cu5 Se1 108.07(4) 2 . ?
Cu5 Cu5 Se1 94.23(7) 5_565 . ?
Cu5 Cu5 Se1 94.23(7) 5_665 . ?
Se4 Cu5 Se1 77.45(4) 6_565 . ?
Cu4 Cu5 Se1 52.21(3) 5_566 . ?
Cu4 Cu5 Se1 52.21(3) 5_666 . ?
Se6 Cu6 Se6 113.54(5) 2_545 2_645 ?
Se6 Cu6 Se3 102.83(3) 2_545 . ?
Se6 Cu6 Se3 102.83(3) 2_645 . ?
Se6 Cu6 Se5 105.88(3) 2_545 . ?
Se6 Cu6 Se5 105.88(3) 2_645 . ?
Se3 Cu6 Se5 126.14(5) . . ?
Se6 Cu6 Cu3 158.34(5) 2_545 2_645 ?
Se6 Cu6 Cu3 70.05(3) 2_645 2_645 ?
Se3 Cu6 Cu3 96.81(4) . 2_645 ?
Se5 Cu6 Cu3 54.10(3) . 2_645 ?
Se6 Cu6 Cu3 70.05(3) 2_545 2_545 ?
Se6 Cu6 Cu3 158.34(5) 2_645 2_545 ?
Se3 Cu6 Cu3 96.81(4) . 2_545 ?
Se5 Cu6 Cu3 54.10(3) . 2_545 ?
Cu3 Cu6 Cu3 98.84(5) 2_645 2_545 ?

_diffrn_measured_fraction_theta_max    1.000
_diffrn_reflns_theta_full              30.00
_diffrn_measured_fraction_theta_full   1.000
_refine_diff_density_max    1.544
_refine_diff_density_min   -2.135
_refine_diff_density_rms    0.683
```